

Supplemental material to

The “tipping” temperature within Subglacial Lake Ellsworth, West Antarctica and its implications for lake access

Malte Thoma,

Klaus Grosfeld, Christoph Mayer, Andrew M. Smith,
John Woodward, and Neil Ross

1. Hydrostatic approximation

Ocean flow modelling is based on the unapproximated (non-hydrostatic) equations of motion on the rotating Earth. Ignoring any source/sink terms they can be written as (e.g., Haidvogel and Beckmann, 1999):

$$\begin{aligned} \frac{d\vec{v}}{dt} + 2\vec{\Omega} \times \vec{v} &= -\frac{\nabla p}{\rho} + \nabla\Phi, \\ \frac{d\rho}{dt} + \rho\nabla \cdot \vec{v} &= 0, \\ \rho c_p \frac{dT}{dt} - \beta T \frac{dp}{dt} &= 0, \\ \frac{dS}{dt} &= 0, \\ \rho &= \rho(T, S, p). \end{aligned}$$

Symbol	Meaning
\vec{v}	velocity
t	time
$\vec{\Omega}$	angular velocity vector
p	pressure
ρ	density
Φ	gravitational potential
c_p	specific heat of water
T	(in situ) temperature
β	thermal expansion coefficient
S	salinity

Not all terms in these equations are of the same order of magnitude. Hence, they can be simplified. In ocean modelling these equations are generally simplified by the *Boussinesq approximation*, the assumption of *incompressibility*, and by the *hydrostatic assumption*. The Boussinesq approximation is valid if variations in density are small compared to its mean value. Incompressibility requires that advective velocities and wave phase speeds are much less than the speed of sound in water, and that the density scale height ($\rho/|\partial\rho/\partial z|$) is much less than the fluid depth (Batchelor, 2000). Within subglacial lake flow modelling these two simplifications are justified. The hydrostatic assumption simplifies the vertical momentum equation, which is generally formulated in spherical coordinates. Following Haidvogel and Beckmann (1999), we present typical scales for ocean and subglacial lake modelling as well as the magnitude of specific terms below:

Scale		Ocean	Lake	Unit	Term	Ocean	Lake	
∂r	$\sim H$	1000	100	m	$\frac{dw}{dt}$	$\sim \frac{U^2 H}{a^2}$	$\mathcal{O}(10^{-11})$	$\mathcal{O}(10^{-18})$
(u, v)	$\sim U$	1	10^{-3}	m/s	$\frac{u^2 + v^2}{a}$	$\sim \frac{U^2}{a}$	$\mathcal{O}(10^{-7})$	$\mathcal{O}(10^{-13})$
w	$\sim UH/a$	10^{-4}	10^{-6}	m/s	$2\Omega u \cos\phi$	$\sim 2\Omega U$	$\mathcal{O}(10^{-5})$	$\mathcal{O}(10^{-9})$
∂t	$\sim a/U$	6500	65000	s	$\frac{\partial p}{\rho \partial z}$	$\sim \frac{p_0}{\rho_0 H}$	$\mathcal{O}(10)$	$\mathcal{O}(100)$
p	$\sim p_0$	10^7	10^7	kg/(m·s ²)	g	$\mathcal{O}(10)$	$\mathcal{O}(10)$	
ρ	$\sim \rho_0$	1000	1000	kg/m ³				
$(d\lambda, d\psi)$	Horiz. dist.	$\mathcal{O}(1)$	$\mathcal{O}(0.1)$	1				
r	Earth radius	$6.5 \cdot 10^6$		m				
Ω	Angular velocity	$7.3 \cdot 10^{-5}$		1/s				

The magnitude of the specified terms indicate that the simplification of the vertical momentum equation by the hydrostatic assumption

$$\frac{1}{\rho_0} \frac{\partial p}{\partial z} + \frac{g\rho}{\rho_0} = 0$$

is justified in subglacial lake modelling. In large-scale flow models, vertical convection is parametrized with a *convective adjustment scheme*. Although it would be interesting to analyse the impact of this simplification, there is currently (to our knowledge) no full 3D-model available that is able to resolve large scale convection on a kilometer scale for realistic geometries.

2. Latent heat

Latent heat (q) is consumed and released by melting and freezing at the lake-ice interface, respectively. The amount is calculated from the density of ice ($\rho_{\text{Ice}} \approx 917 \text{ kg/m}^3$), the specific latent heat of fusion ($L = 334 \text{ kJ/kg}$), and the freezing rate (\dot{m}). Assuming a freezing rate of about $\dot{m} \approx 10 \text{ cm/a}$, the latent heat is about 1 W/m^2 :

$$\begin{aligned} q &= \rho_{\text{Ice}} \cdot L \cdot \dot{m} \\ &\approx 917 \cdot 334 \cdot 10^3 \cdot 10^{-1} \frac{\text{J}}{\text{m}^2 \text{a}} \\ &\approx 30627800 / (3600 \cdot 24 \cdot 365.25) \frac{\text{J}}{\text{m}^2 \text{s}} \\ &\approx 970 \frac{\text{mW}}{\text{m}^2}, \end{aligned}$$

and hence significantly larger than geothermal heating or heat flux into the ice sheet.

3. Measured ice density

During the field campaign (Woodward et al., 2010) a seismic shallow refraction experiment was performed to estimate the ice density of the firn layer up to about 123 m depth (Figure 1). Assuming a constant ice density

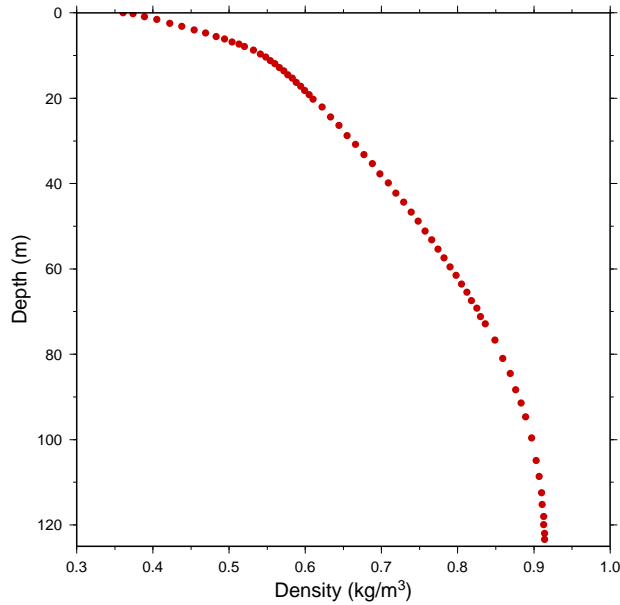


Figure 1: Density–depth relation of the uppermost 125 m in the SLE area.

of $\rho_{\text{Ice}} = 917 \text{ kg/m}^3$ the pressure at $H = 3025 \text{ m}$ depth is $p = \rho_{\text{Ice}} gH \approx 27.21 \text{ MPa}$. Applying the measured density variation of the uppermost 123 m leads to

$$\begin{aligned} p^* &= g \left(\int_{0 \text{ m}}^{123 \text{ m}} \rho_{\text{Ice}} dz + 917 \text{ kg/m}^3 \cdot (3025 \text{ m} - 123 \text{ m}) \right) \\ &= 9.81 \frac{\text{m}}{\text{s}^2} \left(94568.2 \frac{\text{kg}}{\text{m}^2} + 2661134 \frac{\text{kg}}{\text{m}^2} \right) \\ &\approx 27.03 \text{ MPa} \end{aligned}$$

or a pressure-error of about 0.67%. For an ice thickness of 3025 m, this is equivalent to an error of about 20 m. Hence, the critical pressure boundary (tipping depth) would establish in 3045 m depth.

4. Additional Figures

4.1. Circulation in Subglacial Lake Ellsworth

The modelled vertically integrated mass transport stream function in Subglacial Lake Ellsworth indicates two (reversed) gyres of about 0.5 mSv in the deepest part of the lake (Figure 2a). The meridional and zonal transports are slightly weaker as indicated by Figure 2b.

4.2. Sensitivity to ice thickness

The Figures presented in this section illustrate the temperature within the lake (Figure 3–4) as well as the basal mass balance at the lake-ice interface (Figure 5), with respect to different (hypothetically changed) ice thicknesses above the lake. Note that, depending on the ice-lake interface shape and the general ice thickness more than one *Line of Maximum Density* (LOMD) might exist.

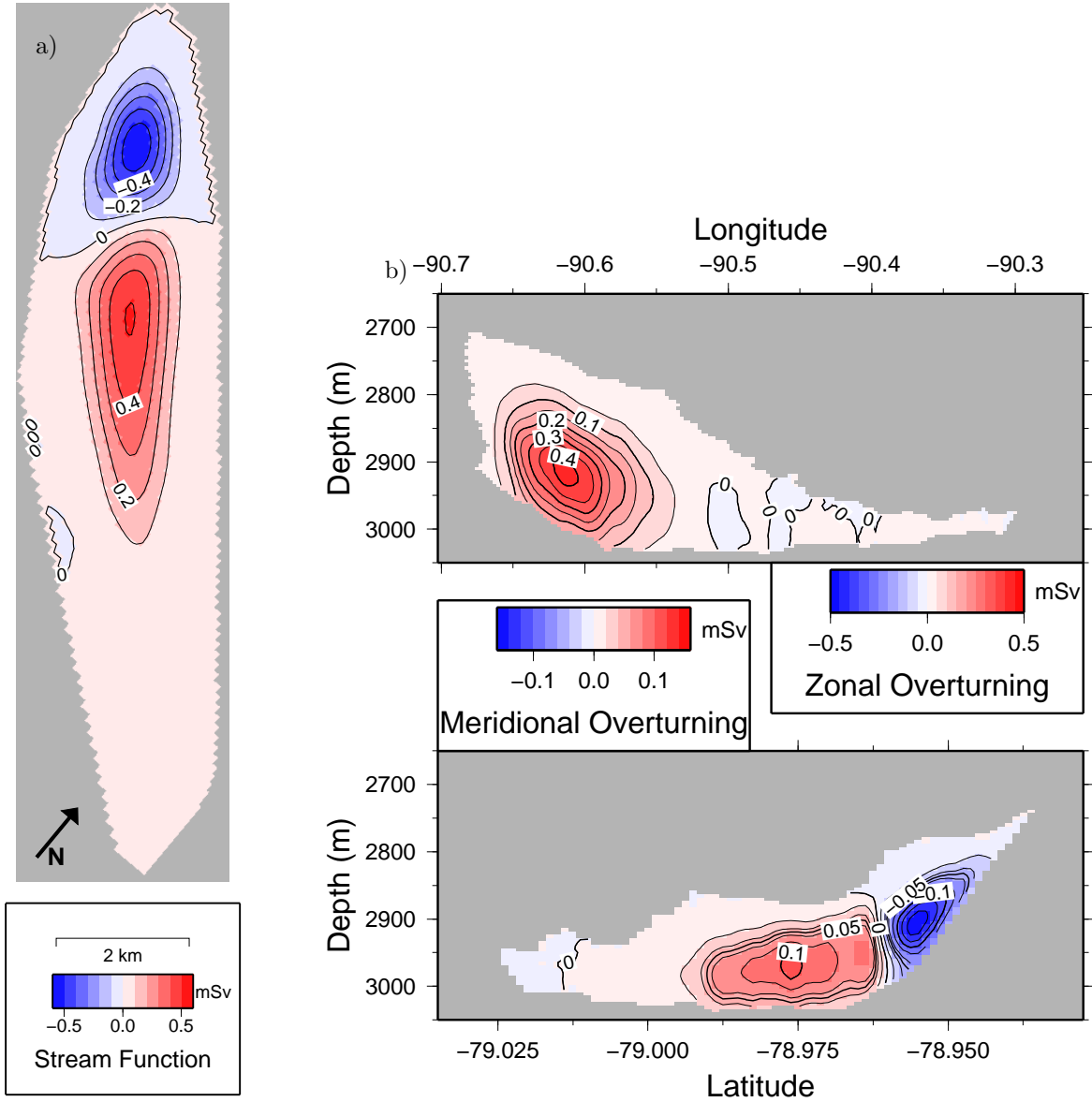


Figure 2: a) Modelled vertically integrated barotropic stream function and b) zonal and meridional overturning circulation within Subglacial Lake Ellsworth ($1 \text{ mSv} = 10^3 \text{ m}^3/\text{s}$).

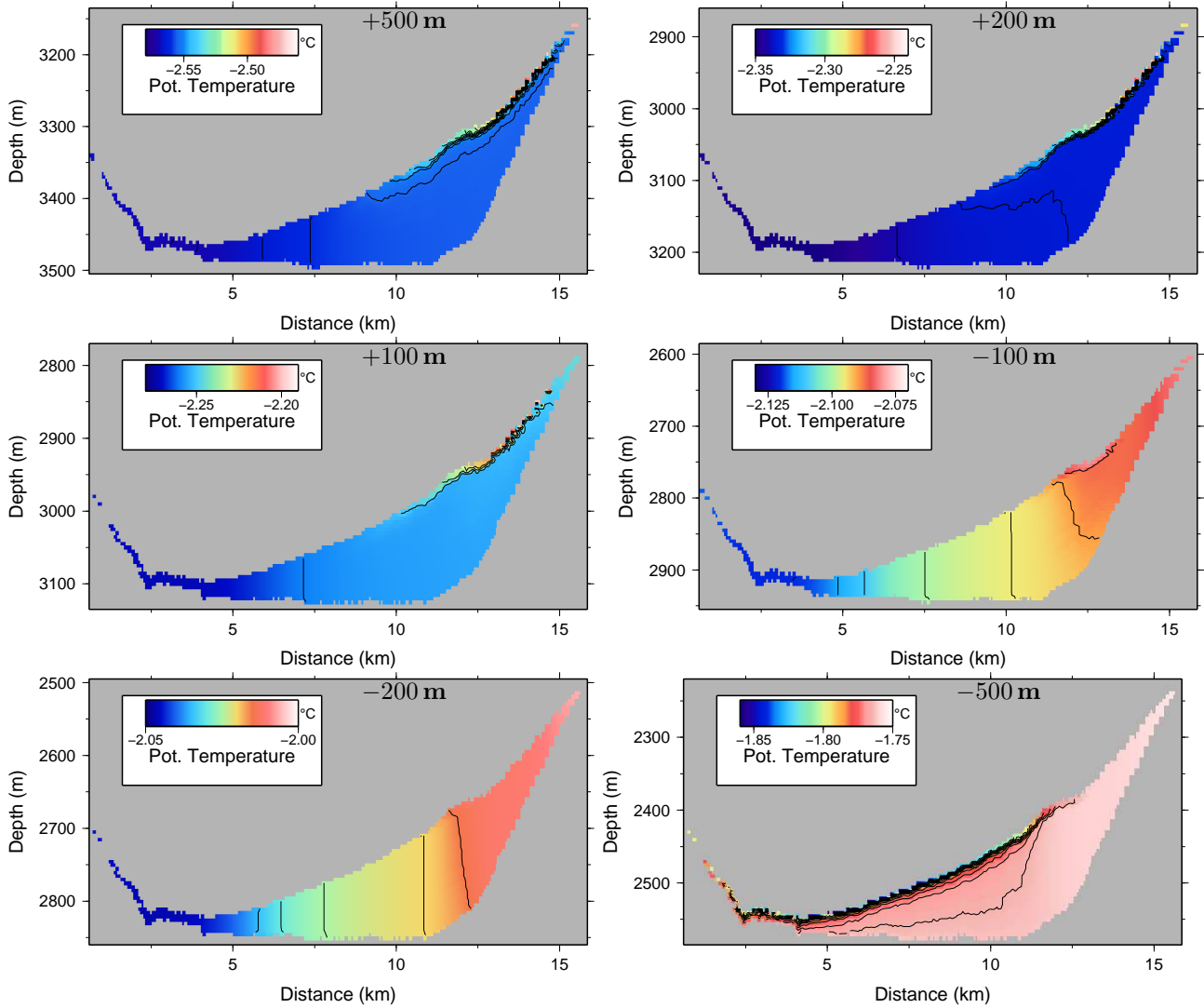


Figure 3: Temperature cross sections along the track indicated in Figure 2a of the corresponding article. The figures indicate the transition of temperature profiles within Subglacial Lake Ellsworth during a (hypothetical) change in ice burden. The individual ice burden is indicated with respect to the present-day situation.

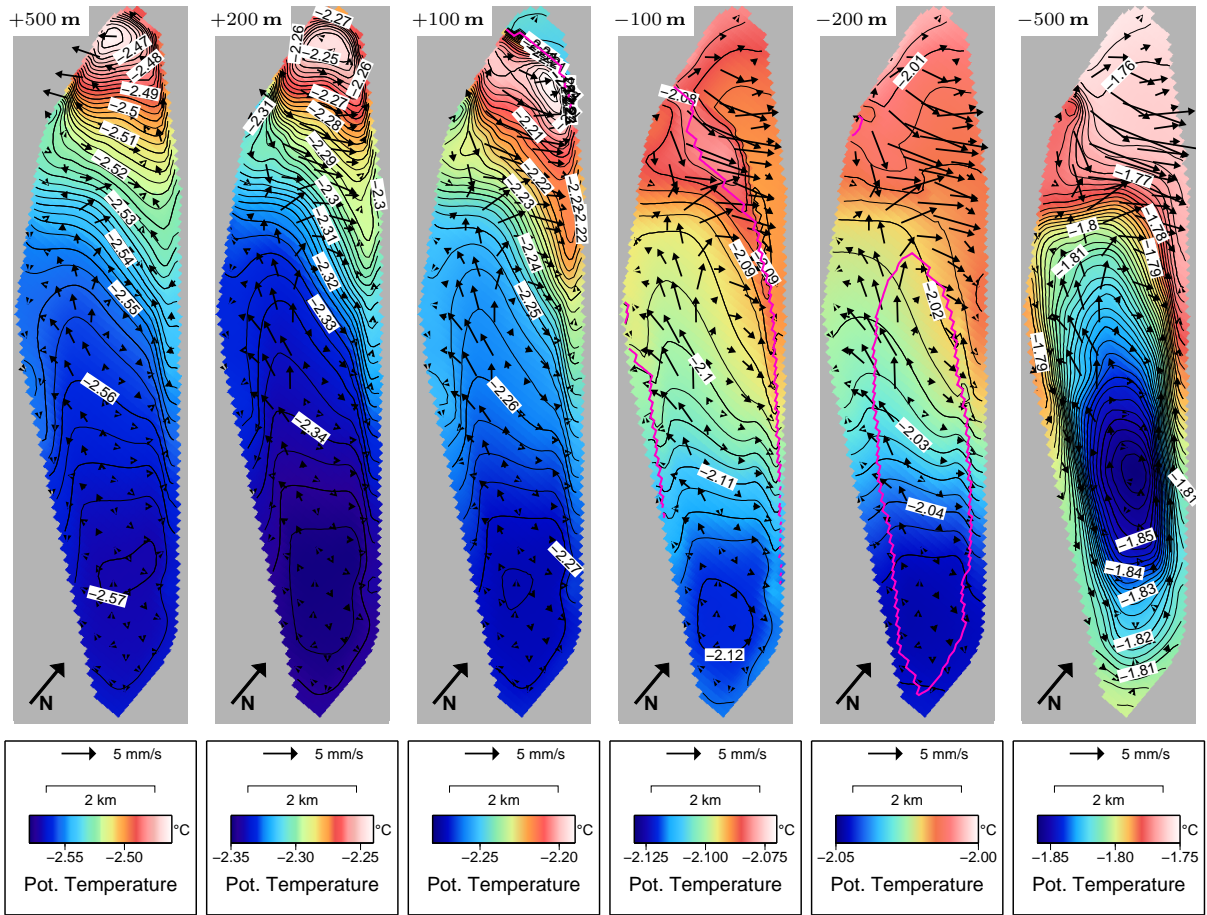


Figure 4: Temperature of the lake-ice interface layer for different ice burdens (see caption of Figure 3). Arrows indicate flow in surface layer. The magenta *tipping lines* (only present for +100 m, -100 m, and -200 m ice burden) indicate where the line of maximum density (LoMD) intersects the lake-ice interface.

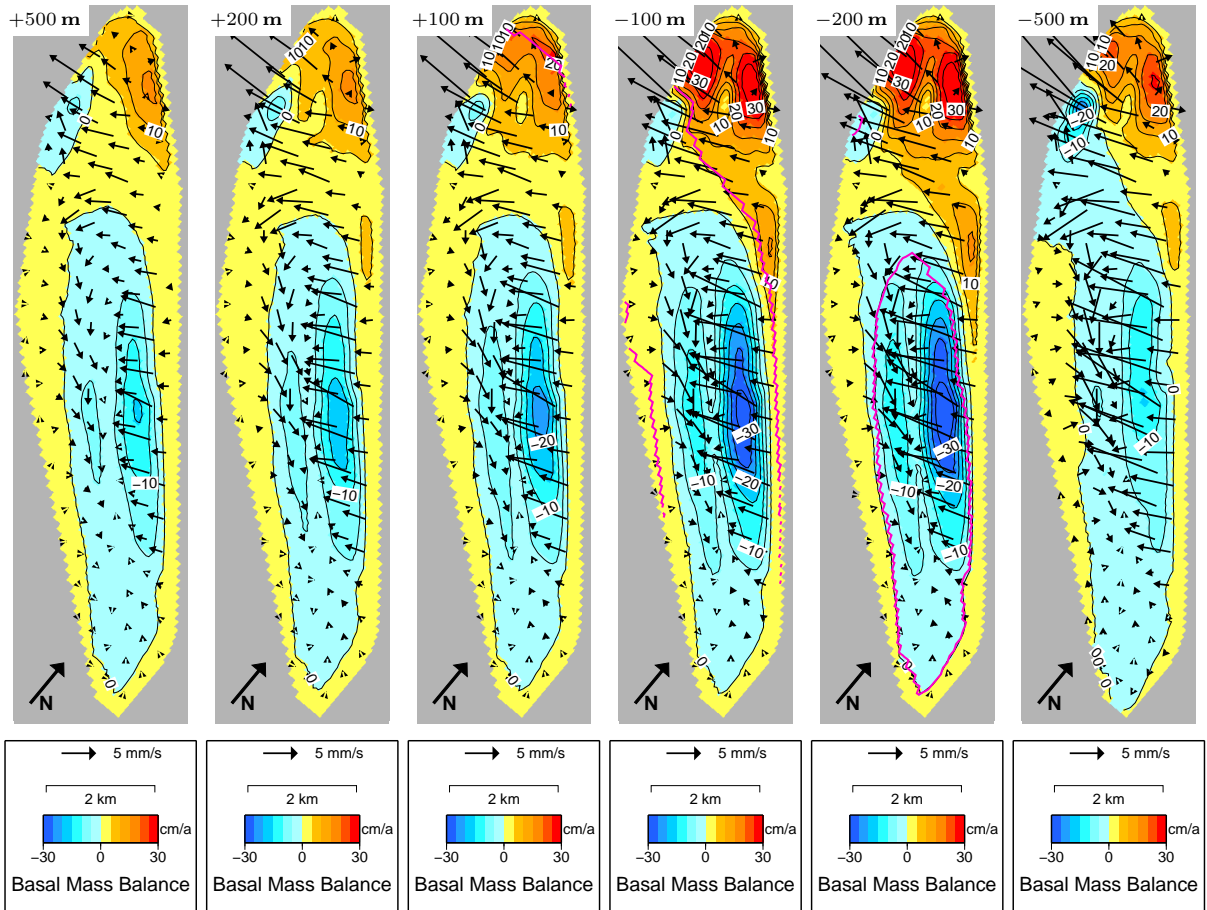


Figure 5: As Figure 4, but for the basal mass balance. Arrows indicate flow in bottom layer.

References

- Batchelor, G. K.: An introduction to fluid dynamics, Cambridge Mathematical Library, 2000.
- Haidvogel, D. B. and Beckmann, A.: Numerical ocean circulation modeling, Imperial Collage Press, London, 1999.
- Woodward, J., Smith, A. M., Ross, N., Thoma, M., Corr, H. F. J., King, E. C., King, M. A., Grosfeld, K., Tranter, M., and Siegert, M. J.: Location for direct access to subglacial Lake Ellsworth: An assessment of geophysical data and modeling, *Geophys. Res. Lett.*, 37, doi:10.1029/2010GL042884, 2010.